

Composition, oxidation, and optical properties of fluorinated silicon nitride film by inductively coupled plasma enhanced chemical vapor deposition

Byung-Hyuk Jun, Joon Sung Lee, and Dae-Weon Kim

Department of Materials Science & Engineering, Korea Advanced Institute of Science and Technology, Kusung-Dong, Yusung-Gu, Taejon, 305-701, Korea

Tae-Hyun Sung

Center for Advanced Studies in Energy and Environment, Korea Electric Power Research Institute, Munji-Dong, Yusung-Gu, Taejon, 305-380, Korea

Byeong-Soo Bae and Kwangsoo No

Department of Materials Science & Engineering, Korea Advanced Institute of Science and Technology, Kusung-Dong, Yusung-Gu, Taejon, 305-701, Korea

(Received 30 March 1998; accepted 24 June 1998)

Amorphous fluorinated silicon nitride films have been deposited with the variation of NF_3 flow rate using SiH_4 , N_2 , Ar, and NF_3 gases by inductively coupled plasma enhanced chemical vapor deposition for the first time, and the absolute composition, oxidation mechanism, and optical properties were investigated. The absolute composition including hydrogen was performed by means of elastic recoil detection time of flight. It was found that the oxygen and fluorine contents in the film dramatically increased, but the hydrogen content decreased to below 4 at.% as the NF_3 flow rate increased. The oxidation mechanism could be explained in terms of the incorporation of the activated residual oxygen species in the chamber into the film with unstable open structure by the fluorine-added plasma. It was shown that the density and optical properties such as refractive index, absorption coefficient, and optical energy gap depended on the film composition. The variations of the above properties for fluorinated silicon nitride film could be interpreted by the contents of fluorine and oxygen with high electronegativity.

I. INTRODUCTION

Many studies of the silicon nitride films in microelectronics have been made for applications such as a passivation layer, intermetal dielectric, and gate insulator for semiconductor technology. Although these films are called silicon nitride, they are not stoichiometric compound Si_3N_4 but amorphous hydrogenated silicon nitride ($a\text{-SiN}_x\text{:H}$) films. Conventionally, $a\text{-SiN}_x\text{:H}$ films are prepared at a relatively low temperature of 300 °C by plasma enhanced chemical vapor deposition (PECVD) using SiH_4/NH_3 or $\text{SiH}_4/\text{NH}_3/\text{N}_2$ gas mixtures. These films usually contain as much as 25–35% of hydrogen¹ which is incorporated in the network structure in the form of Si–H and N–H bonds. The impurities can produce localized states in the band gap of the dielectrics which are electrically active as deep trapping or recombination centers. Therefore, these $a\text{-SiN}_x\text{:H}$ films exhibit inferior electrical properties as well as poor resistance to chemical attack.

Many attempts have been made to optimize the hydrogen content and the local bonding configurations in $a\text{-SiN}_x\text{:H}$ films.^{2–5} Among the studies, one approach is to substitute the stronger Si–F bond (116 kcal/mol)

for the weaker Si–H bond (71.4 kcal/mol)⁶ in the network using fluorine-added source. Since the amorphous fluorinated silicon nitride ($a\text{-SiN}_x\text{:F}$) film exhibits better resistance against hydrogen diffusion, better electrical properties, and higher thermal stability compared to amorphous silicon nitride film, it could be a substitute of SiN_x film.^{2–4} Moreover, the applicability as a bottom antireflective layer (BARL) in quarter-micron optical lithography was already revealed by controlling film thickness and optical constants such as refractive index and extinction coefficient.⁷

In this study, an inductively coupled plasma (ICP)⁸ enhanced CVD system, as a kind of remote PECVD type producing high plasma density of typically 10^{11} – 10^{12} ions/cm³, was adopted for the first time for fabricating the $\text{SiN}_x\text{:F}$ films using SiH_4 , N_2 , Ar, and NF_3 gases. Conventional fluorine-free silicon nitride film was also fabricated and was used as a reference. This system can offer easy composition control as well as a considerable reduction in surface damage imposed on the substrate and can reduce the content of impurity-like hydrogen compared to conventional parallel PECVD.⁹

Accurate composition analysis should be preceded to comprehend the film properties. However, there have been no methods to perform the absolute quantitative analysis for the light elements such as N, O, F, and H of below atomic number 10. Especially, in the case of hydrogen, it has been the only way to use the area of the Fourier transform infrared (FTIR) absorption of the Si–H and N–H peaks (near 2200 and 3360 cm^{-1} , respectively) by the Lanford model,¹⁰ but applying this method is tenuous and may tend to overestimate the hydrogen content. In this paper, the elastic recoil detection time of flight (ERD-TOF) technique for absolute quantitative analysis including hydrogen of the fluorinated silicon nitride films will be presented. Then, the variations of the film optical properties such as the refractive index (n), absorption coefficient (α), and optical energy gap (E_{opt}) will be interpreted with the film composition obtained by this new powerful technique. It has been reported that the SiN_x :F films with fluorine above 10 at.% are unstable when exposed to air.⁴ The presence of fluorine in these films has been believed to induce hydrolysis leading to oxygen incorporation.^{4,11} However, another oxidation mechanism for the films deposited here will be discussed.

II. EXPERIMENTAL DETAILS

The fluorinated silicon nitride films were fabricated using ICP enhanced CVD system, and a schematic diagram of this system for the deposition is shown in Fig. 1. ICP source uses RF coil around the plasma chamber to couple power inductively to the plasma through the alumina chamber wall. The films were deposited on *p*-type (100) Si and fused silica substrates simultaneously using SiH_4 , N_2 , Ar, and NF_3 gases. In order to reduce the hydrogen content in the film, N_2 gas was used instead of NH_3 as a nitrogen source. As presented in Fig. 1, the N_2 , Ar, and NF_3 gases are fed from a showerhead being in the center of the water-cooled flange into the plasma chamber, and SiH_4 gas is directly introduced into the reaction chamber through a gas ring. These gases were fed after the chamber, and lines were evacuated to the base pressure of 3 mTorr, which was the minimum pressure available in this study because only a rotary pump with the capacity of 1000 l/min was used, and the film deposition was done under the pressure of about 250 mTorr by controlling the auto pressure controller (APC) valve. The activated gases formed the fluorinated silicon nitride film on the substrates located on a susceptor which could be rotated, moved up/down, and heated up to a maximum 700 °C by a resistant heater. The deposition conditions are listed in Table I.

The compositional analysis of the films deposited on Si substrate was performed by the ERD-TOF method

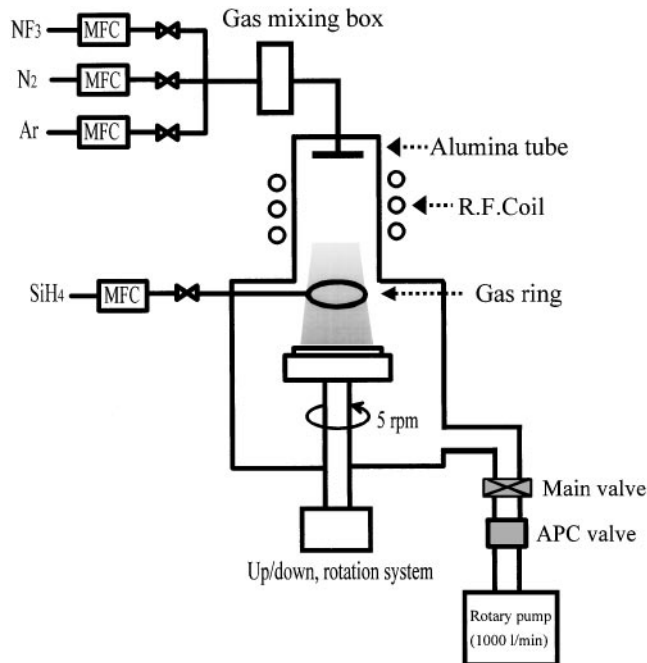


FIG. 1. A schematic diagram of ICP enhanced CVD system.

TABLE I. Deposition conditions of fluorinated silicon nitride film.

| | |
|--|---|
| Substrate | <i>p</i> -type (100) Si and fused silica |
| Base pressure | 3 mTorr |
| Working pressure | About 250 mTorr |
| RF power | 250 W |
| Deposition temperature | 300 °C on Si, 250 °C on fused silica |
| NF_3 flow rate | 0, 0.5, 0.75, 1, 1.5, 2 sccm |
| $[\text{SiH}_4 : \text{N}_2 : \text{Ar} =$ | |
| 2 : 15 : 150 (sccm)] | |
| Film thickness | About 90–100 nm on Si About 110–120 nm on fused silica |

using the $^{35}\text{Cl}^{+5}$ ion of an acceleration energy of 9.622 MeV as an incident beam. This measurement technique is two-dimensional detection measuring the flight time as well as the energy of recoiled elements and is a powerful method in analyzing absolute composition of light elements including hydrogen below atomic number 10 when compared to conventional Rutherford backscattering spectroscopy (RBS). The film density could be calculated with total atom numbers recoiled from the whole film thickness per cm^2 and measured film thickness. The oxidation mechanism of the film was investigated using an Auger electron spectroscopy (AES) depth profile for the structure of $\text{SiN}_x/\text{SiN}_x$:F/Si substrate. In AES detection, the electron acceleration voltage and the current were 5 kV and 300 nA, respectively, and Ar sputtering voltage and current density were 3 kV and 250 $\mu\text{A}/\text{cm}^2$, respectively. The refractive index at the wavelength of 633 nm and the thickness for the film deposited on Si substrate were

evaluated by an ellipsometer. The thickness of the film deposited on fused silica substrate was measured with α -step. The transmittance and reflectance of the films deposited on fused silica substrate were measured using a Shimadzu UV-3101 PC UV-VIS-NIR scanning spectrophotometer, and the absorption coefficient and optical energy gap were calculated from this data and film thickness.

III. RESULTS AND DISCUSSION

A. Absolute composition; ERD-TOF analysis

The thin film x-ray diffraction (TFXRD) analysis showed that all deposited films had x-ray amorphous phases. The variation of absolute composition of the films deposited on Si substrate with NF_3 flow rate was analyzed using an ERD-TOF method. Figures 2(a) and 2(b) show the energy versus flight time spectra for the films deposited using NF_3 flow rates of 0.5 sccm and 1.5 sccm, respectively. The oxygen and fluorine signals increase as the NF_3 flow rate increases from 0.5 sccm to 1.5 sccm. That is, the oxygen incorporation is enhanced together with increasing fluorine content in the films. Even though neither oxygen gas nor precursor containing oxygen was used in the deposition, oxygen was detected in the spectrum. This phenomenon will be discussed in the next section. From the energy versus time spectra, each element can be converted to the energy axis without overlapping between light elements. With the count height designated as a line fit in energy versus count spectrum, the absolute quantitative analysis could be done in a similar way to RBS. Figure 3 represents the composition variation for each element of the films deposited at different NF_3 flow rates. Most of the films are Si-rich phases. As the NF_3 flow rate increases from 0.5 sccm to 2 sccm, the oxygen and fluorine contents in the film increase up to 22.4 at.% and 11.2 at.%, respectively, while the hydrogen content decreases to below 4 at.%. The hydrogen content decreases due to the active decomposition of SiH_4 gas and the active formation of HF by-product with increasing NF_3 flow rate.²

The variation of the densities of the $\text{SiN}_x\text{:F}$ films with NF_3 flow rates obtained from ERD-TOF analysis and film thickness measurement is shown in Fig. 4. The density of the $\text{SiN}_x\text{:F}$ film decreases from 2.32 g/cm^3 to 2.07 g/cm^3 by the decrease of silicon content with relatively heavy mass, which compares with $1.5\text{--}2.8 \text{ g/cm}^3$ for other fluorinated silicon nitride films prepared by PECVD.^{3,11} The density of the $\text{SiN}_x\text{:F}$ film is significantly lower than that of the conventional high temperature thermal CVD Si_3N_4 , which is about 3.24 g/cm^3 . However, it is comparable with that of the fluorine-free normal $\text{SiN}_x\text{:H}$ film deposited here, which is about 2.31 g/cm^3 .

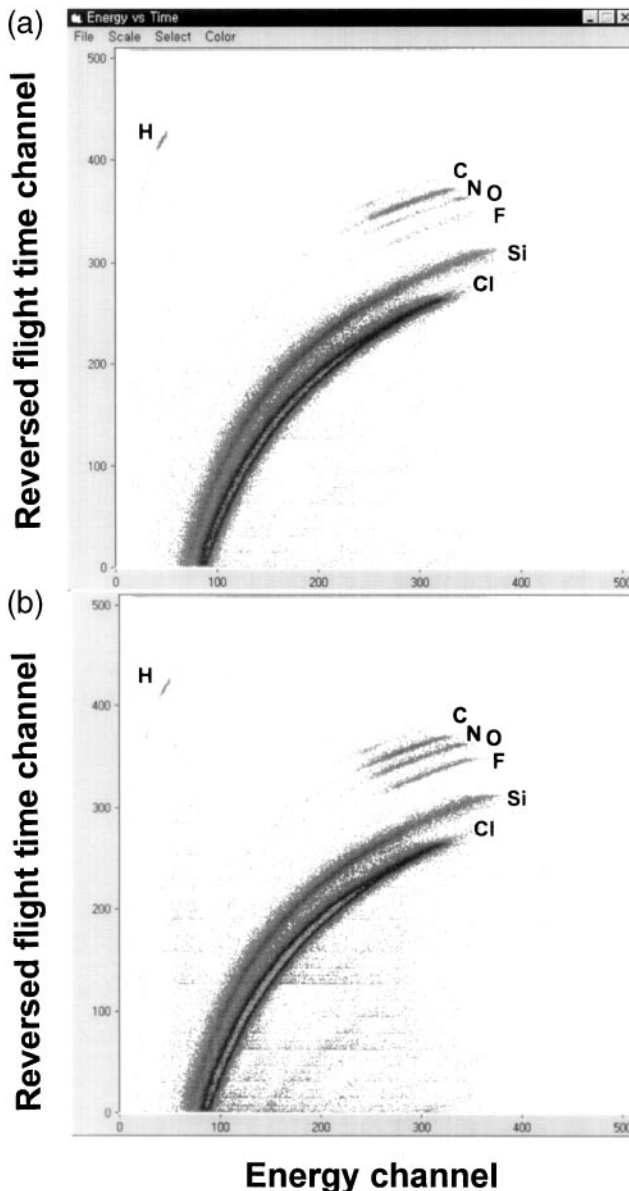


FIG. 2. Energy versus time spectra by ERD-TOF of fluorinated silicon nitride films deposited at 250 mTorr, 250 W, 300 °C, $\text{SiH}_4\text{:N}_2\text{:Ar} = 2\text{:}15\text{:}150$ (sccm) and NF_3 flow rates of (a) 0.5 sccm and (b) 1.5 sccm.

B. Oxidation mechanism

It has been reported that the oxygen incorporation in the film could be explained by the hydrolysis mechanism of the fluorine-contained films.^{11–13} According to the study of Sanchez *et al.*,^{11,13} under the 80% moisture atmosphere, the film with high fluorine content as $[-\text{SiF}_2-]_n$ presents an open structure which favors the penetration of water and oxygen molecules into the network. Although the $[-\text{SiF}_2-]_n$ chain concentration is initially stable due to the structural characteristics, it gradually produces silicon oxide and ammonium hexafluorosilicate $[(\text{NH}_4)_2\text{SiF}_6]$, which is the decomposed

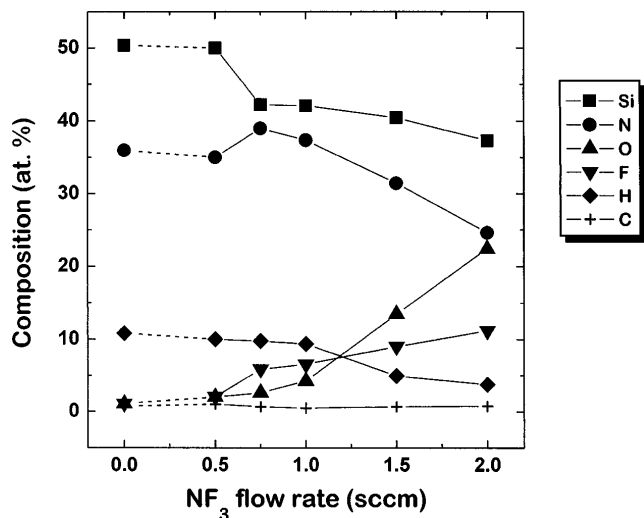


FIG. 3. Composition variation with the NF_3 flow rate of fluorinated silicon nitride film using ERD-TOF [250 mTorr, 250 W, 300 °C, and $\text{SiH}_4 : \text{N}_2 : \text{Ar} = 2 : 15 : 150$ (sccm)].

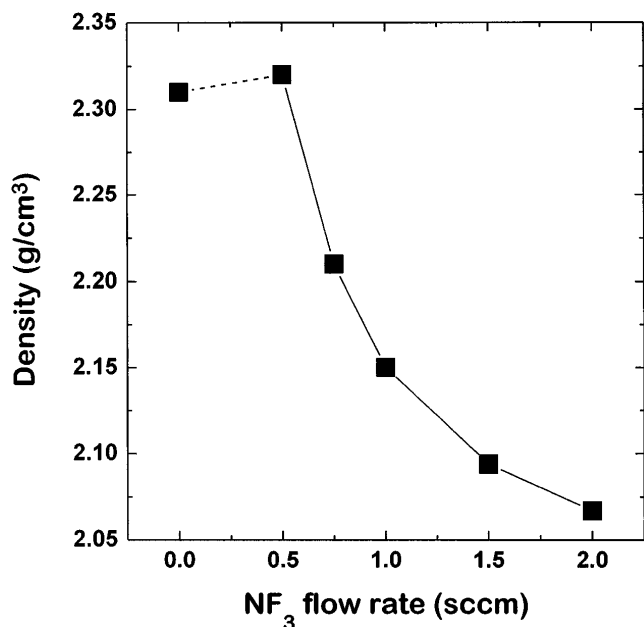


FIG. 4. Film density variation with the NF_3 flow rate of fluorinated silicon nitride film [250 mTorr, 250 W, 300 °C, and $\text{SiH}_4 : \text{N}_2 : \text{Ar} = 2 : 15 : 150$ (sccm)].

form of the additional compound at humid condition for a long time. Also, Livengood *et al.*⁴ reported that the fluorinated silicon nitride film containing fluorine greater than 10 at.% in the film was almost completely oxidized after air exposure for four months. The films showing atomic ratio $\text{F}/\text{Si} > 0.5$ with $\text{N}/\text{Si} < 1.1$ are oxidized in air atmosphere and water as observed by Chang *et al.*¹²

Although the fluorinated silicon nitride films prepared in this study had the atomic ratio of $\text{F}/\text{Si} < 0.3$

(max. 11.2 at.% F) with $\text{N}/\text{Si} < 0.92$, the films kept a stable state for a long time. This was confirmed by the fact that the values of the refractive indices and thicknesses of the films exposed to air for above six months were maintained to be constant. Still more, any complete oxidation for all films deposited in this study did not occur. As shown in Fig. 3, the continuous increase of oxygen content in the film with increasing NF_3 flow rate is detected.

In order to examine the possible cause of oxygen incorporation in the film, the silicon nitride film as a passivation layer was *in situ* deposited on the fluorinated silicon nitride film prepared with relatively high NF_3 flow rate under the condition of 250 mTorr, 250 W, 300 °C, and $\text{SiH}_4 : \text{N}_2 : (\text{NF}_3) : \text{Ar} = 2 : 15 : (1.5) : 150$ (sccm). And then, AES depth analysis was performed for the SiN_x (150 nm)/ $\text{SiN}_x : \text{F}$ (90 nm)/Si substrate. Figure 5 shows AES depth profile magnified for carbon, oxygen, and fluorine elements. This indicates the peak-to-peak intensity obtained from AES spectra with the film depth, which cannot represent the absolute contents of the elements. When compared to absolute contents of O and F elements in Fig. 3, it seems that the content of oxygen is much higher than that of fluorine. Generally, in Ar sputtering of AES depth analysis, it is well known that the fluorine element is more volatile than the oxygen element due to the difference of bond strengths (see Table II⁶). Therefore, the fluorine content coming into the AES detector after Ar sputtering is relatively lower than real value when compared to oxygen. On the other hand, the result of Fig. 3 obtained by ERD-TOF measurement means absolute composition with little content loss in detection. As shown in Fig. 5, the oxygen is incorporated in the only $\text{SiN}_x : \text{F}$ film

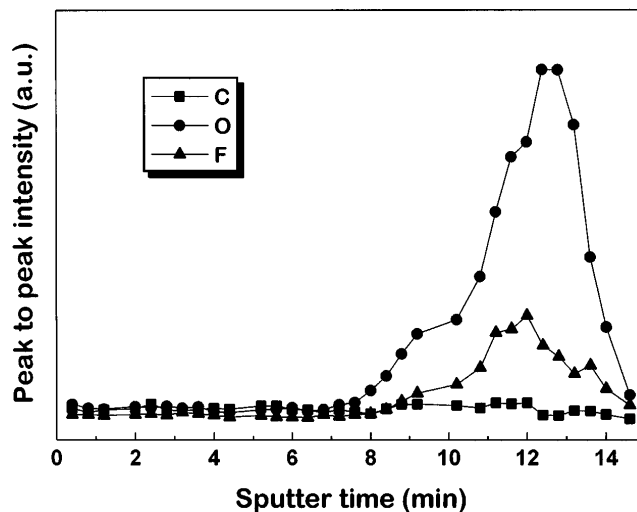


FIG. 5. AES depth profile for SiN_x (150 nm)/ $\text{SiN}_x : \text{F}$ (90 nm)/Si structure *in situ* deposited at 250 mTorr, 250 W, 300 °C, and $\text{SiH}_4 : \text{N}_2 : (\text{NF}_3) : \text{Ar} = 2 : 15 : (1.5) : 150$ (sccm).

region. This observation tells us that the oxidation of the films occurs not by the hydrolysis but by the effect of fluorine-added plasma in the deposition chamber. It seems that the activated residual oxygen species in the deposition chamber due to using only rotary pump are incorporated into the film with the open structure due to the fluorine element. This was certified by the fact that the refractive index of the film prepared at 250 mTorr, 250 W, 300 °C, $\text{SiH}_4 : \text{N}_2 : \text{Ar} = 2 : 15 : 150$ (sccm) and very high NF_3 flow rate of 5 sccm was 1.46, which was similar to that of silicon dioxide film, and AES analysis showed the film consisted of mostly Si and O with small F.

The activated oxygen species take part in the deposition and combine with Si element. As shown in Table II, the bond strength of Si–O in the film is stronger than those of N–O and F–O and is the largest compared to Si–N and Si–F. On the other hand, the bond strength of Si–F is much higher than those of N–F or O–F. Therefore, most oxygen and fluorine atoms may exist in the forms of Si–O and Si–F bonds rather than being bonded to nitrogen. These bonding configurations of fluorine-contained silicon nitride film were already revealed by FTIR studies.^{5,12,13} Therefore, the open structure of $[-\text{SiF}_2-]_n$ in the $\text{SiN}_x : \text{F}$ film can be filled and stabilized by the oxygen element during the plasma deposition, and the films keep stabilizing after air exposure.

C. Deposition rate and refractive index

The deposition rate and refractive index at the wavelength of 633 nm of the films deposited at various NF_3 flow rates in the range of 0–2 sccm are shown in Fig. 6. As the NF_3 flow rate increases, the deposition rate increases continuously from 37 Å/min ($\text{NF}_3 : 0$ sccm) to 88 Å/min ($\text{NF}_3 : 2$ sccm). Generally, the deposition rate significantly increases with the addition of the NF_3 gas compared to the case of silicon nitride film. It seems that the reaction between activated species by the addition of NF_3 gas occurs more actively.

The refractive indices of fluorinated silicon nitride films decrease from 2.21 to 1.62 consistently by the increase of oxygen and fluorine contents with increasing the NF_3 flow rate from 0.5 to 2 sccm. The refractive index at the wavelength of 633 nm of the conventional amorphous Si_3N_4 film is about 2.02, but the value (2.5) observed for silicon nitride film ($\text{NF}_3 : 0$ sccm) in this study is relatively high due to Si-rich phase as mentioned in the composition analysis. The refractive

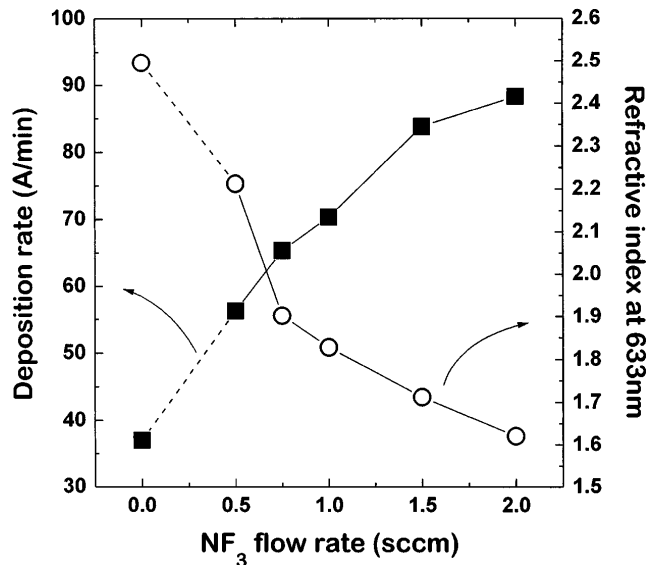


FIG. 6. Effect of NF_3 flow rate on the deposition rate and refractive index of fluorinated silicon nitride film [250 mTorr, 250 W, 300 °C, and $\text{SiH}_4 : \text{N}_2 : \text{Ar} = 2 : 15 : 150$ (sccm)].

index is related to the electronic polarization of the atom or ion which is proportional to the atomic or ionic volume.¹⁴ The electronegativity values of the fluorine and oxygen atoms are greater than that of nitrogen. [cf. Electronegativity (Pauling value): Si = 1.9, N = 3.04, O = 3.44, F = 3.98]. The greater electronegativities of both fluorine and oxygen give rise to lower ionic volume, and then cause lower polarizability.¹⁴ Thus, the refractive index decreases due to the increase of the contents of oxygen and fluorine with high electronegativity.

D. Absorption coefficient and optical energy gap

The effect of NF_3 flow rate on the optical properties such as absorption coefficient and optical energy gap is investigated for the films deposited on fused silica substrate. Although the deposition temperature and film thickness are dependent on the substrate as mentioned in Table I, it was verified by ERD-TOF measurement that a film composition on fused silica substrate was almost the same as that on Si substrate prepared together.

Based on the transmittance and reflectance data, the absorption coefficient (α) as a function of the wavelength can be obtained by the following equation:

$$T = (1 - R)^2 \exp(-\alpha d), \quad (1)$$

where the T and R are the transmittance and reflectance, respectively, and d is the film thickness. In the high absorption portion of the uv absorption edge, the absorption coefficient for amorphous semiconductors is found to obey the following relation suggested by Mott and Davis¹⁵:

$$\alpha h\nu = B(h\nu - E_{\text{opt}})^n, \quad (2)$$

TABLE II. Bond strengths between each element (kcal/mol).

| | | | | | |
|------|-----|-----|-------|------|------|
| Si–N | 105 | N–F | 62.6 | H–Si | 71.4 |
| Si–F | 116 | O–F | 56 | H–N | 75 |
| Si–O | 184 | O–N | 150.8 | H–F | 136 |

where B is constant, $h\nu$ is the photon energy, and E_{opt} is optical energy gap. Mott and Davis proposed that most amorphous semiconductors have allowed direct transitions, and n in Eq. (2) is 2, as also proposed by Tauc¹⁶ under the assumption of parabolic bands. The optical energy gap (E_{opt}) values are obtained from Eq. (2) by extrapolation of the linear parts of the $(\alpha h\nu)^{1/2}$ versus $h\nu$ curves to $(\alpha h\nu)^{1/2} = 0$.

Figure 7 shows the optical absorption spectra of the $\text{SiN}_x:\text{F}$ films deposited at the various NF_3 flow rates. As the NF_3 flow rate increases, the absorption edge shifts to shorter wavelength since the electron transition in the band gap is more difficult due to the increase of the contents of oxygen and fluorine ions with high electronegativity. Thus, it is expected that the optical energy gap grows with the increment of NF_3 flow rate. The variation of the film optical energy gaps with the NF_3 flow rates obtained from Eq. (2) is shown in Fig. 8. As the NF_3 flow rate increases from 0.5 sccm to 2 sccm, the E_{opt} increases from 2.8 to 5.7 eV continuously as expected. For reference, the E_{opt} values of amorphous SiN_x , SiO_xN_y films, and $\text{SiN}_x:\text{F}$ films are in the ranges of 2.5–5.6 eV^{2,17} and 4.9–5.6 eV,^{5,12,17} respectively, depending on the composition.

IV. CONCLUSIONS

The amorphous fluorinated silicon nitride thin films have been fabricated on Si and fused silica substrates using SiH_4 , N_2 , Ar, and NF_3 gases by ICP enhanced CVD process, and the effect of NF_3 flow rate on the absolute composition, oxidation mechanism, and optical properties was investigated. The absolute quantitative analysis for all elements in the films was performed by

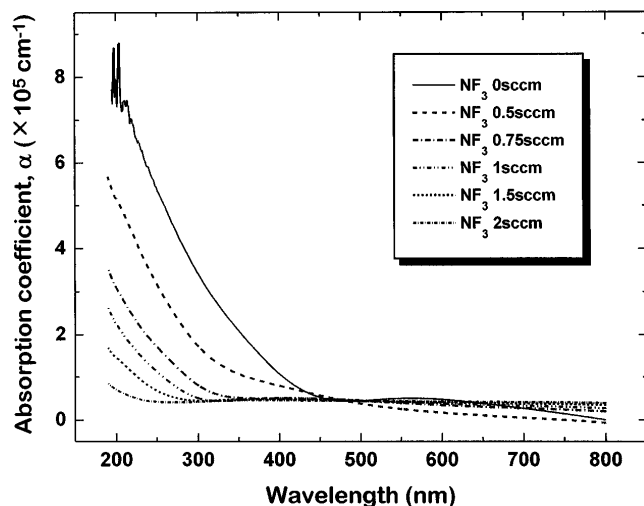


FIG. 7. Effect of NF_3 flow rate on the absorption coefficient as a function of wavelength of fluorinated silicon nitride film [fused silica substrate, 250 mTorr, 250 W, 250 °C, and $\text{SiH}_4:\text{N}_2:\text{Ar} = 2:15:150$ (sccm)].

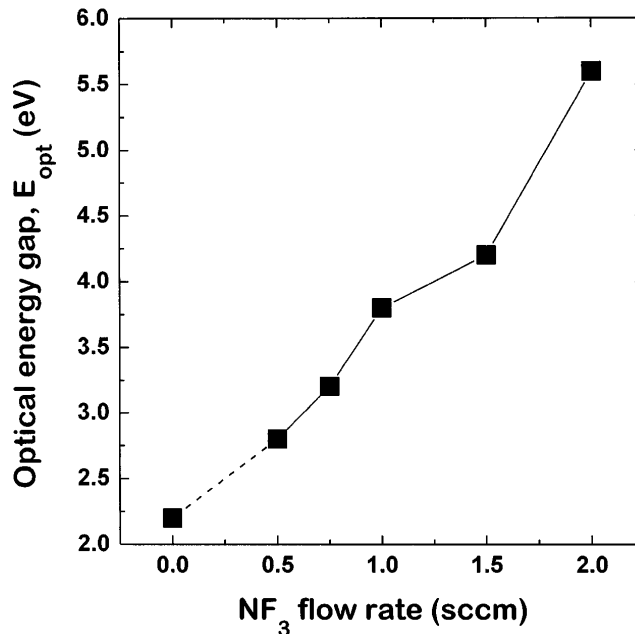


FIG. 8. Effect of NF_3 flow rate on the optical energy gap of fluorinated silicon nitride film [fused silica substrate, 250 mTorr, 250 W, 250 °C, and $\text{SiH}_4:\text{N}_2:\text{Ar} = 2:15:150$ (sccm)].

ERD-TOF measurement. As the NF_3 flow rate increases from 0.5 sccm to 2 sccm, the fluorine content in the film continuously increases, but the hydrogen content decreases to below 4 at.%. Extraordinarily, although the oxygen gas is not fed, the oxygen content in the film dramatically increases to 22 at.% with the increase of NF_3 flow rate. It was proved by *in situ* deposition of SiN_x film on $\text{SiN}_x:\text{F}$ film deposited with a relatively high NF_3 flow rate of 1.5 sccm that the oxidation was due to the incorporation of the residual oxygen species into the film with unstable open structure by the fluorine-added plasma.

These oxygen and fluorine have higher electronegativities among the constituent elements, and thus it has great influence on the film properties. The density of the $\text{SiN}_x:\text{F}$ film decreases from 2.32 to 2.07 g/cm^3 with the decrease of silicon content by increasing the NF_3 flow rate from 0.5 to 2 sccm. The refractive index at the wavelength of 633 nm decreases from 2.21 to 1.62 consistently because of the increase of the contents of oxygen and fluorine with high electronegativity. Based on the transmittance and reflectance data of the films deposited on fused silica substrate, the absorption coefficient as a function of the wavelength for the various NF_3 flow rates was calculated, and then the optical energy gap was obtained. As the NF_3 flow rate increases 0.5 to 2 sccm, the absorption edges occur at shorter wavelengths, and thus E_{opt} increases with wide range from 2.8 to 5.7 eV continuously due to the weak band

gap transition of electron by increasing the contents of oxygen and fluorine elements.

ACKNOWLEDGMENTS

The authors thank Dr. J.K. Kim in Korea Institute of Geology, Mining and Materials for valuable assistance in the ERD-TOF measurement. This study was supported by the academic research fund of Ministry of Education, Republic of Korea, through Inter-University Semiconductor Research Center (ISRC 97-E-1024) in Seoul National University.

REFERENCES

1. A. J. Lowe, M. J. Powell, and S. R. Elliott, *J. Appl. Phys.* **59**, 1251 (1986).
2. S. Fujita and A. Sasaki, *J. Electrochem. Soc.* **135**, 2566 (1988).
3. N. Watanabe, M. Yoshida, Y-C. Jiang, T. Nomoto, and I. Abiko, *Jpn. J. Appl. Phys.* **30**, L619 (1991).
4. R. E. Livengood and D. W. Hess, *Appl. Phys. Lett.* **50**, 560 (1987).
5. S. Fujita, H. Toyoshima, and A. Sasaki, *J. Appl. Phys.* **64**, 3481 (1988).
6. *Thermodynamic and Kinetic Data in CRC Materials Science and Engineering Handbook*, edited by J.F. Shackelford, W. Alexander, and J.S. Park (CRC, Boca Raton, FL, 1994), p. 93.
7. B-H. Jun, S-S. Han, D-W. Kim, H-Y. Kang, Y-B. Koh, B-S. Bae, and K. No, in *Amorphous and Crystalline Insulating Thin Films IV*, edited by W. Warren, R. Devine, M. Matsumura, S. Cristoloveanu, Y. Homma, and J. Kanicki (Mater. Res. Soc. Symp. Proc. **446**, Pittsburgh, PA, 1997), pp. 115–120.
8. M.A. Lieberman and A.J. Lichtenberg, *Principles of Plasma Discharges and Materials Processing* (John Wiley & Sons, New York, 1994), p. 387.
9. G. Lucovsky, D.V. Tsu, and R.J. Markunas, in *Handbook of Plasma Processing Technology*, edited by S.M. Rossnagel, J.J. Cuomo, and W.D. Westwood (Noyes, Park Ridge, NJ, 1990), p. 387.
10. W. A. Lanford and M. J. Rand, *J. Appl. Phys.* **49**, 2473 (1978).
11. C. Gomez-Aleixandre, O. Sanchez Garrido, and J.M. Albella, *J. Vac. Sci. Technol. B* **8**, 540 (1990).
12. C-P. Chang, D.L. Flamm, D.E. Ibbotson, and J.A. Mucha, *J. Appl. Phys.* **62**, 1406 (1987).
13. O. Sanchez, C. Gomez-Aleixandre, and C. Palacio, *J. Vac. Sci. Technol. B* **11**, 66 (1993).
14. M. W. Barsoum, *Fundamentals of Ceramics*, edited by B. J. Clark and J. M. Morriss (McGraw-Hill, Singapore, 1997), p. 526.
15. N.F. Mott and E.A. Davis, *Electronic Processes in Non-Crystalline Materials* (Clarendon, Oxford, 1979), p. 272.
16. J. Tauc, in *Optical Properties of Solids*, edited by F. Abeles (North-Holland, Amsterdam, 1970), p. 277.
17. V. A. Gritsenko, in *Silicon Nitride in Electronics (Materials Science Monographs, Vol. 34)*, edited by A. V. Rzhano (Elsevier, Amsterdam, 1988), p. 154.